Stem Cell Reports, Volume *8*

Supplemental Information

DIDO as a Switchboard that Regulates Self-Renewal and Differentiation in Embryonic Stem Cells

Agnes Fütterer, Jésus de Celis, Rosana Navajas, Luis Almonacid, Julio Gutiérrez, Amaia Talavera-Gutiérrez, Cristina Pacios-Bras, Ilenia Bernascone, Fernando Martin-Belmonte, and Carlos Martinéz-A

Supplemental Information

Supplemental Figures

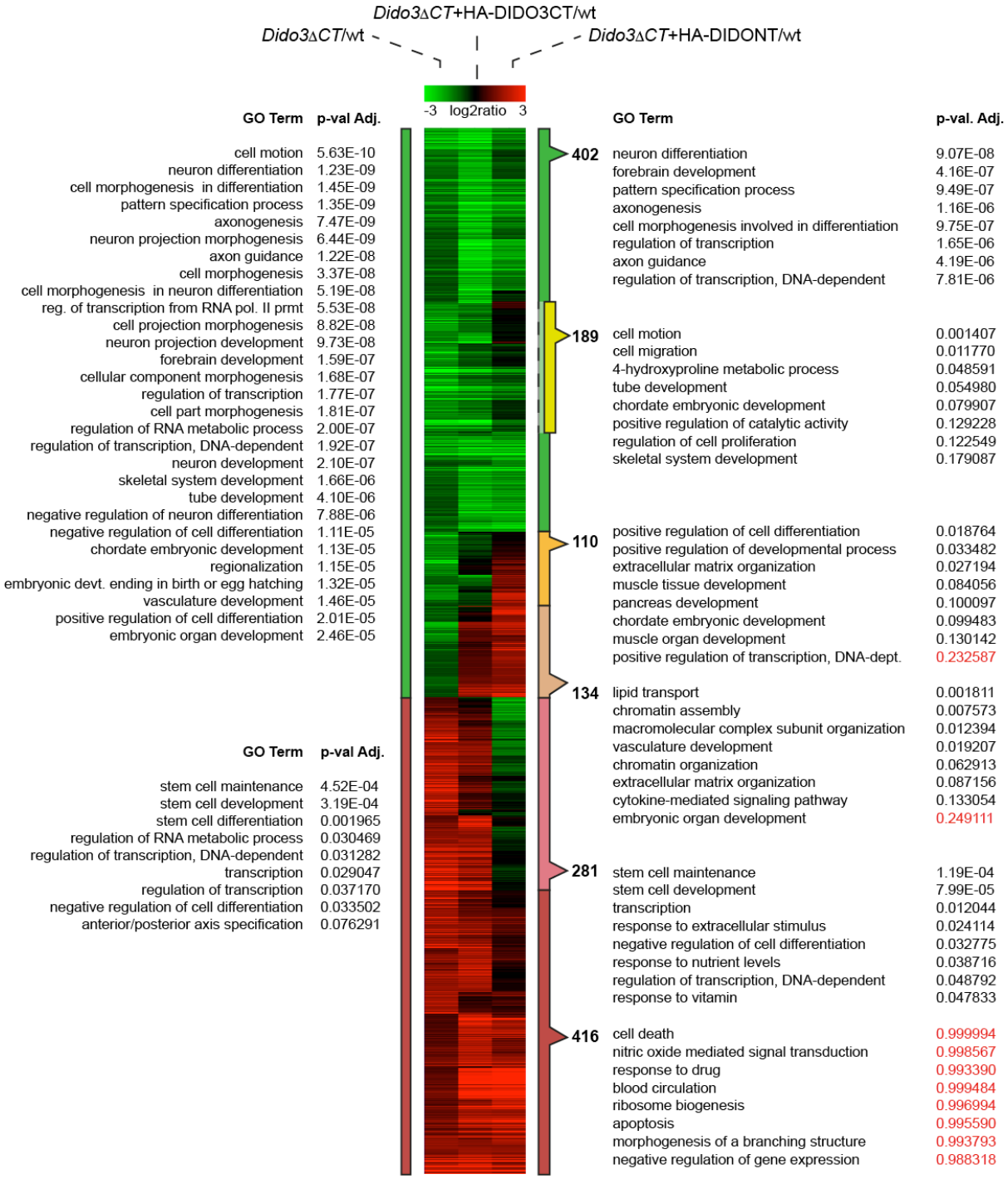

Figure S1. ***Functional effect of DIDO domain expression in Dido3ΔCT day 10 embryoid bodies (d10EB).*** **Related to Figure 1.** Complete results and GO analysis of Agilent microarray data for d10EB from *Dido3ΔCT* (left), *Dido3ΔCT*+HA-DIDO3CT (center) and *Dido3ΔCT*+HA-DIDONT (right) cells vs wt.

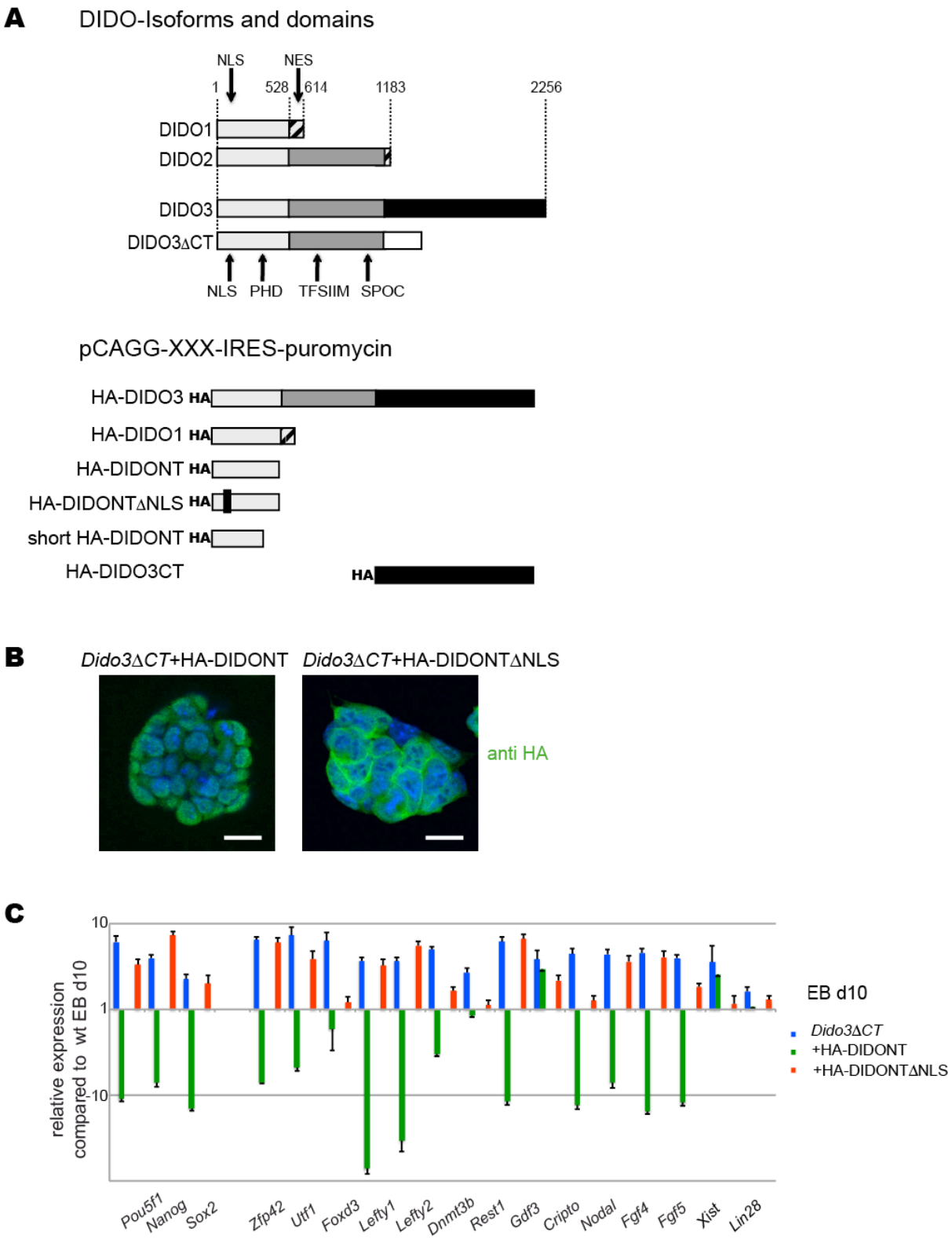

Figure S2. ***Scheme of DIDO domains and expression vectors and effect of HA-DIDONTΔNLS expression on Dido3ΔCT day 10 embryoid bodies (d10EB).*** **Related to Figure 1.** (**A**) Top, scheme of DIDO isoforms and their conserved domains, nuclear localization site (NLS) and nuclear export signal (NES). Bottom, HA-tagged plasmids used for ectopic expression of DIDO regions. (**B**) Top, labeling of embryonic stem cells (ESC) with anti-HA (green) for cellular localization of HA-DIDONT (nucleus) vs HA-DIDONTΔNLS (cytoplasm). Nuclear counterstaining (DAPI, blue). Scale bars, 20 μm. (**C**) Bottom, relative expression compared to wt (baseline) of selected stemness markers for d10EB from *Dido3ΔCT* (blue bars), *Dido3ΔCT*+HA-DIDONT reconstituted (green bars) and *Dido3ΔCT*+HA-DIDONTΔNLS (red bars) determined by qRT-PCR. Data shown as mean ± SEM, $n = 3$.

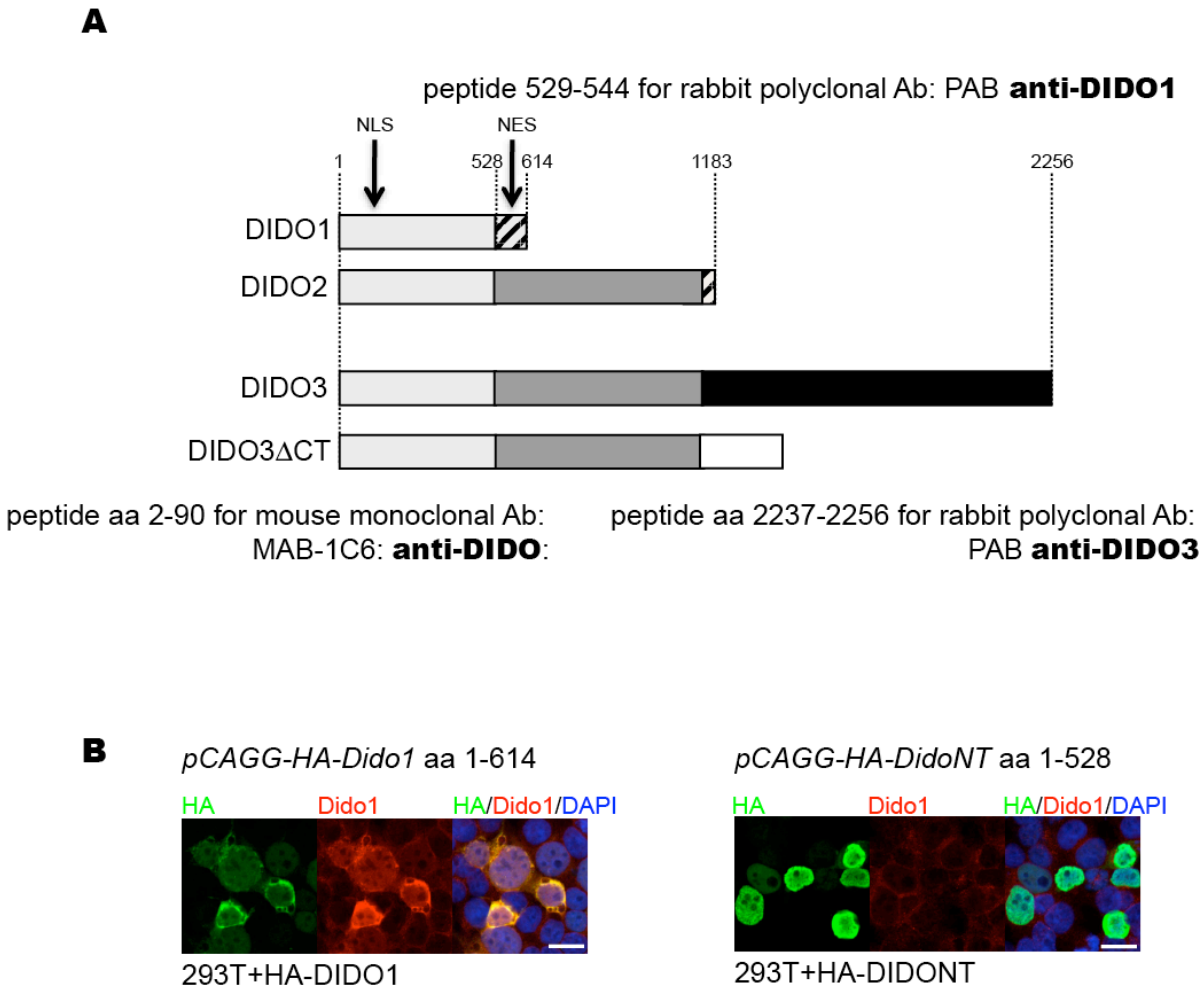

Figure S3. ***Details of different anti-DIDO isoform antibodies.*** **Related to Figure 2.** (**A**) Generation of anti-DIDO MAB-1C6 using the DIDO common N-terminal peptide, originally termed anti-CAS (common amino-terminal segment) (Prieto et al., 2009), of the polyclonal PAB-DIDO1 and PAB-DIDO3, each using isoform-specific C-terminal peptides; PAB-DIDO3 was previously described (Trachana et al., 2007). (**B**) Control staining for PAB-DIDO1 (red). Left, 293T cells expressing HA-DIDO1 with overlapping staining for PAB-DIDO1 (red) and anti-HA (green). Right, 293T cells expressing HA-DIDONT positive only for anti-HA (green). Nuclear counterstaining with DAPI (blue). Scale bars, 20 μm.

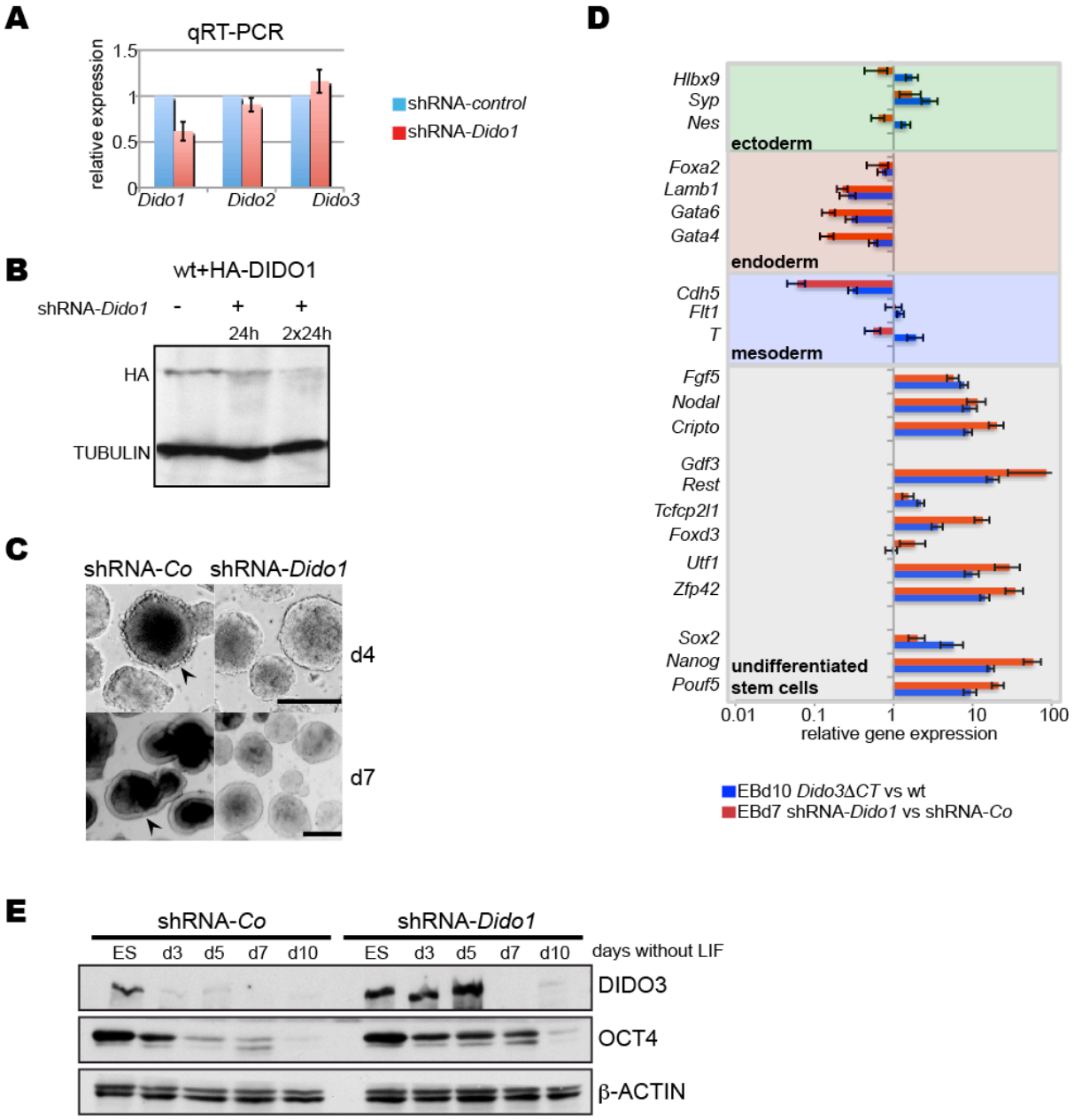

Figure S4. ***Additional controls for impaired differentiation capacity of shRNA-Dido1 ESC.*** **Related to Figure 3.** (**A**) Relative expression of *Dido* isoforms 1, 2 and 3, comparing shRNA-*control* cells (expression 1) and shRNA-*Dido1* cells determined by qRT-PCR. Data show mean ± SEM, $n = 3$. (**B**) shRNA-*Dido1* specificity confirmed in a western blot of wt cells with ectopic HA-DIDO1 expression; western blot developed with anti-TUBULIN as loading control. (**C**) Light microscopy images of d4- (top) and d10EB (bottom) of shRNA-*control* (left) and shRNA-*Dido1* (right) EB. Arrows indicate primitive endoderm in d4EB and further differentiation signs in d7EB. Scale bars, 100 μm. (**D**) Quantitative RT-PCR was used to determine the relative expression of selected markers for undifferentiated ESC, as well as endoderm, mesoderm and ectoderm in differentiating EB. d10EB of *Dido3ΔCT* (blue bars) and d7EB of shRNA-*Dido1* EB (red bars) were compared to wt or shRNA-*control* EB (baseline), respectively. Data show mean ± SEM, $n = 3$. (**E**) Expression of DIDO3 (top) and OCT4 (center) in lysates of ESC and of a d3-10EB time course in shRNA-*control* (left) vs shRNA-*Dido1* cells (right); β-ACTIN was used as loading control (bottom).

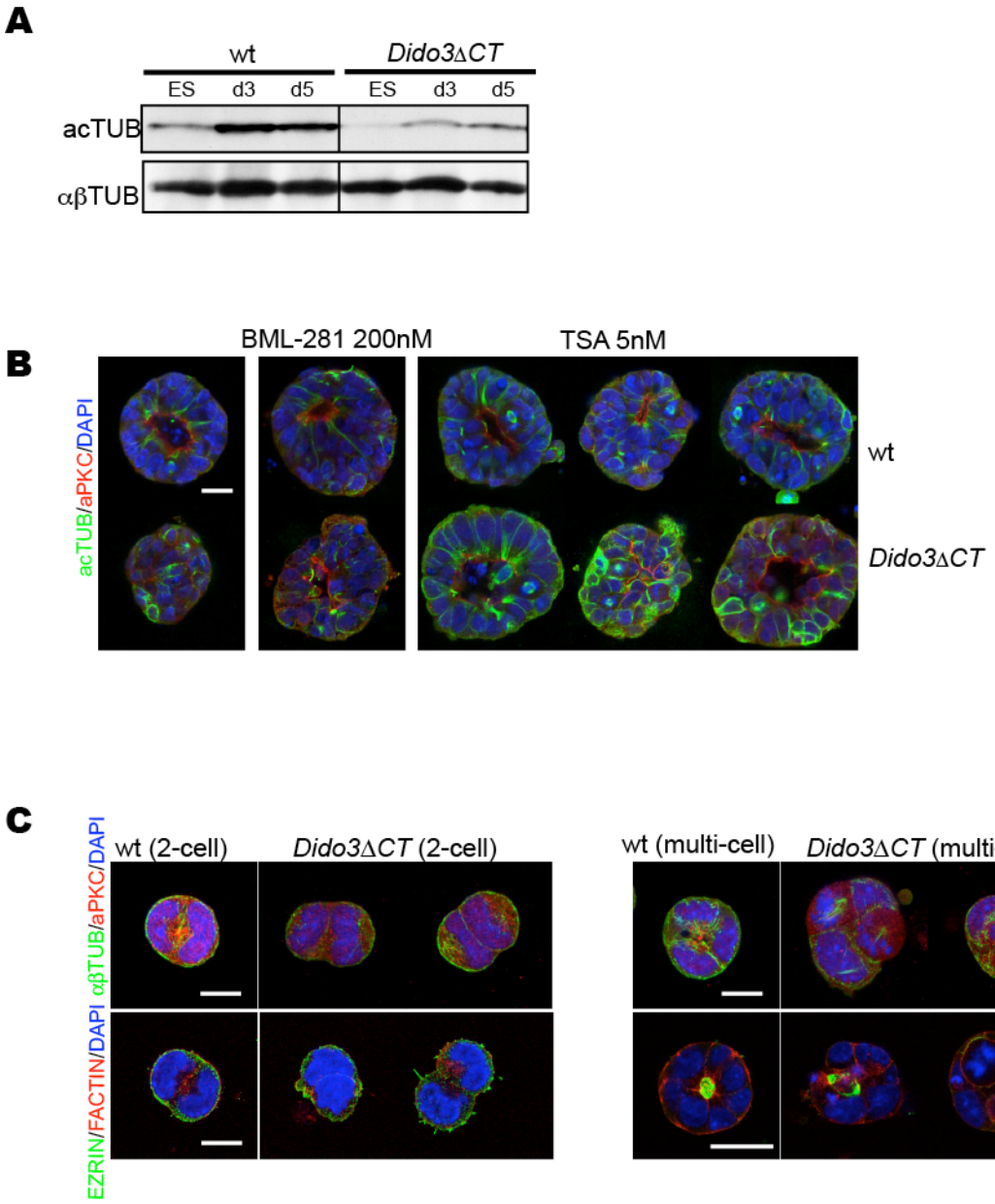

Figure S5. ***TUBULIN acetylation and organization in EB and rosettes.*** **Related to Figure 4.** (**A**) Western blot analysis of wt *vs Dido3ΔCT* lysates of ESC, d3EB and d5EB developed with anti-acetylated TUBULIN (top) or total -αβ-TUBULIN (bottom). (**B**) Treatment of rosettes with two HDAC inhibitors (untreated (left), BML-281-treated (center), or trichostatin (TSA)-treated (right)), rosettes of wt ESC (top) or *Dido3ΔCT* ESC (bottom) were stained with anti-acetylated TUBULIN (green) and -aPKC (red). (**C**) Comparison of wt vs *Dido3ΔCT*. Top, TUBULIN organization (green) and aPKC localization (red) in two-cell (left) and multi-cell rosettes (right); bottom, lumen formation marker EZRIN (green) and phalloidin label of F-ACTIN (red) of two-cell (left) and multi-cell (right) rosettes. (B,C) Nuclear counterstaining with DAPI (blue). Scale bars for 2-cell rosettes, 10 μm, multi-cell rosettes, 20 μm.

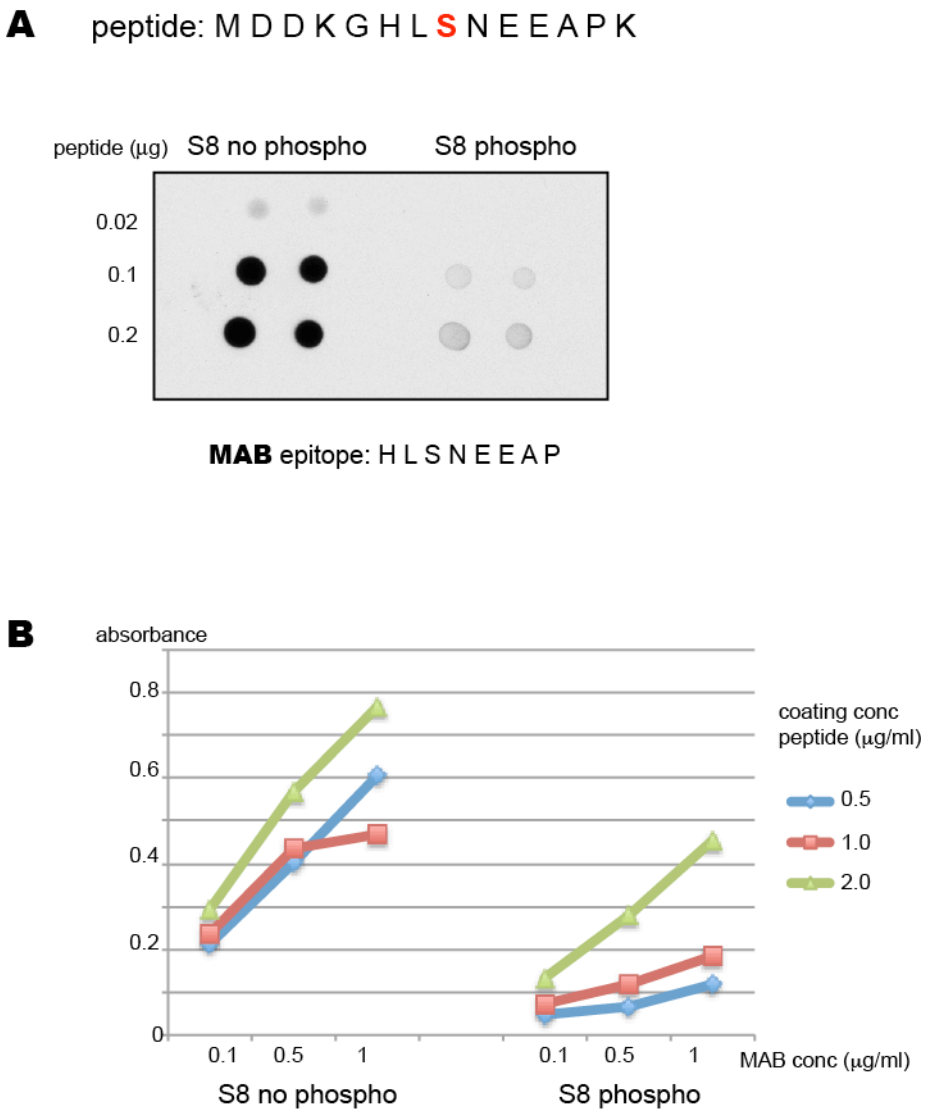

Figure S6. ***Epitope characterization of anti-DIDO MAB-1C6.*** **Related to Figure 5.** (**A**) Dot-blot analysis with MAB-1C6 for binding affinity to its epitope, which is dependent on phosphorylation on S8. We used the unphosphorylated (left) and S8-phosphorylated (right) peptides; both were dotted on nitrocellulose at three concentrations and developed with MAB-1C6 as for a standard western blot. (**B**) Standard ELISA procedure was used to test binding affinity of MAB-1C6 to both peptides (unphosphorylated *vs* S8-phosphorylated); different concentration combinations of antibody and coating peptides were tested.

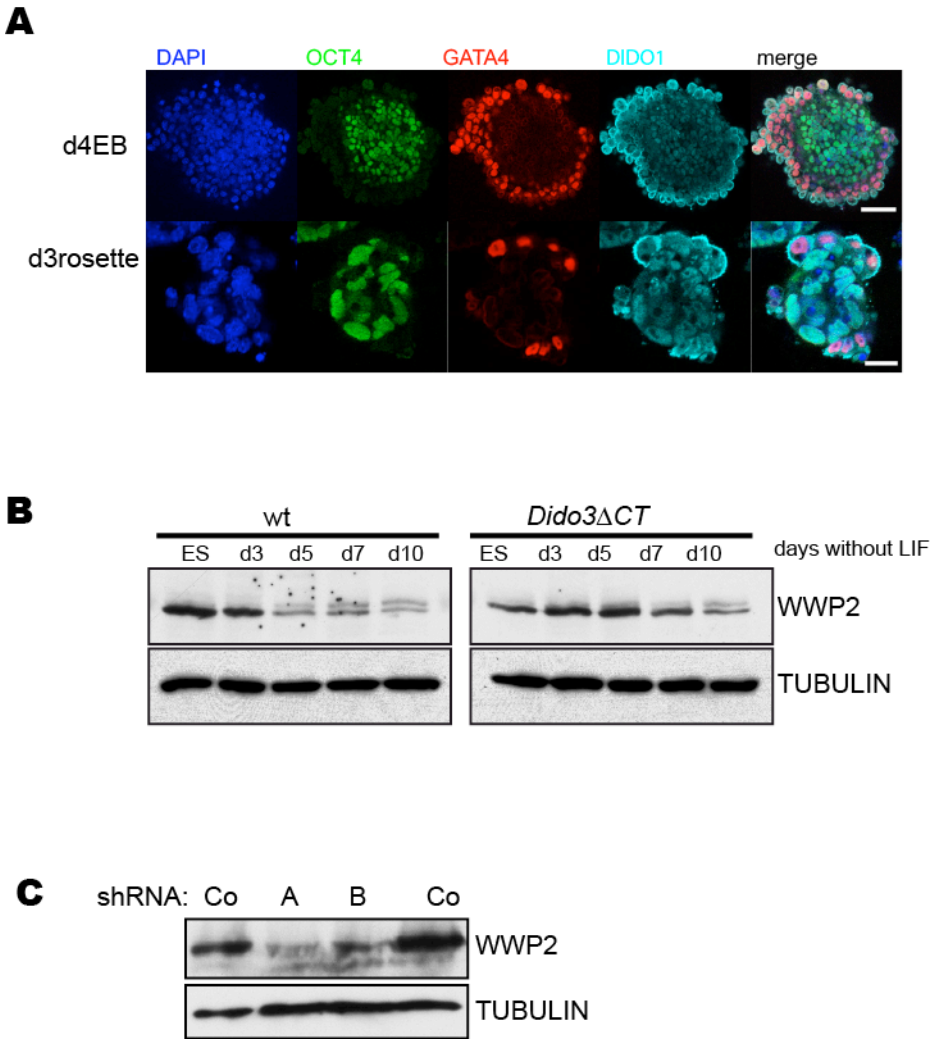

Figure S7. ***Cell fate markers of primitive endoderm (PE) and shRNA-Wwp2 controls.*** **Related to Figure 6.** (**A**) Characteristic staining pattern for PE cells in d4EB (top) and d3rosettes (bottom) with anti-OCT4 (green, negative in PE cells, positive inside EB), anti-GATA4 (red, positive only in PE cells), anti-DIDO1 (cyan, positive at apical membrane of PE cells and weak nuclear staining); nuclear counterstaining with DAPI (blue). Scale bars for EB, 50 μm; rosettes, 20 μm. (**B**) WWP2 expression in lysates of ESC and of a d3-10EB time course. Western blot analysis of wt (left) vs *Dido3ΔCT* (right) with anti-WWP2 (top) and -TUBULIN (bottom; loading control). (**C**) Top, WWP2 expression in shRNA-*control vs* two clones of shRNA-*Wwp2* A and B ESC. Bottom, loading control with anti-TUBULIN.

Table S1. ***Differentially expressed genes in EBd10 of Dido3ΔCT, Dido3ΔCT expressing HA-DIDO3CT or HA-DIDONT, all vs wt EBd10 with p <0.05, FDR <0.2 and fold change >2.*** **Related to Figure 1.**
RNA from three biological replicates was analyzed in Agilent microarrays. Data were normalized and filtered as described in Supplemental Experimental Procedures (below). Only statistically significant differentially expressed genes are shown.

Table S2. ***Gene lists used for GO analysis of differentially expressed probes in EBd10 of Dido3ΔCT, Dido3ΔCT reconstituted with HA-DIDO3CT or HA-DIDONT, all vs wt EBd10 2.*** **Related to Figure 1.** List of probes used for gene ontology enrichment analysis from Agilent microarrays of EBd10 (see Supp Table S2). Only GO biological process terms are described. Gene lists were created from HCL (hierarchical clustering) of statistically filtered data (see Supplemental experimental Procedures below).

Table S3, ***Differentially expressed genes of Dido3ΔCT ESC vs wt ESC with p <0.05, FDR <0.2 and fold change >2.*** **Related to Figure 2.** RNA from three biological replicates was analyzed in Affymetrix microarrays. Data were normalized and filtered as mentioned in Supplemental Experimental Procedures (below). Only statistically significant differentially expressed genes are shown.

Table S4. ***List of significant genomic intervals of ChIP-seq for HA-DIDO3 in ESC.*** **Related to Figure 7.**
Significant peaks were called by MACS v1.4 software, comparing experimental sample vs input. Eight peaks were identified for the *Dido* gene (in bold).

Supplemental Experimental Procedures

Microarrays

Affymetrix microarrays

RNA target preparation

Mouse embryonic stem cell cultures were harvested, snap-frozen in liquid nitrogen, and stored at -80°C. Total RNA was extracted using the guanidinium isothiocynate method (TRIzol reagent; Invitrogen, Carlsbad, CA), followed by purification using an RNeasy column (Qiagen, Valencia, CA). Each RNA preparation was tested for degradation using the Agilent 2100 Bioanalyzer (Agilent Technologies, Palo Alto, CA). cDNA was synthesized from 4 μg total RNA using One-Cycle target labeling and control reagents (Affymetrix, Santa Clara, CA) to produce biotin-labeled cRNA. The cRNA preparations (10 μg) were fragmented (94ºC, 35 min) into 35-200 bases in length.

Affymetrix microarray processing

GeneChip Mouse Genome 430 2.0 Array processing (hybridization, washing and scanning). Fragmented cRNA (10 μg) was hybridized to the mouse MOE 430 2.0 array (Affymetrix) containing 39000 transcript variants from 34000 well-characterized mouse genes. Each sample was added to hybridization solution containing 100 mM 2-(N-morpholino)ethanesulfonic acid, 1 M Na^+, and 20 mM EDTA, with 0.01% Tween-20 to a final cRNA concentration of 0.05 μg/ml. Hybridization was performed for 16 h at 45ºC. Each microarray was washed and stained with streptavidin-phycoerythrin in a Fluidics station 450 (Affymetrix) and scanned at 1.56 μm resolution in a GeneChip Scanner 3000 7G System (Affymetrix). Images were acquired and analyzed using GeneChip Operating Software (GCOS). Microarray processing, hybridization and initial statistical analysis were performed by the Genomics Facility at the Centro Nacional de Biotecnología.

Agilent microarray

RNA target preparation

Mouse embryoid bodies were harvested at day 10, snap-frozen in liquid nitrogen, and stored at -80°C. Total RNA was extracted using the guanidinium isothiocynate method (TRIzol reagent; Invitrogen), followed by purification using an RNeasy column (Qiagen). RNA quality was assessed using the Agilent Model 2100 Bioanalyzer (Agilent Technologies). For microarray use, 10 μg of total RNA was processed.

Agilent microarray processing

Agilent Mouse GE 4x44K v2 V2 (G4852A-028005). Array processing (hybridization, washing and scanning)
This microarray array is comprised of >44000 probe sets that interrogate 39430 transcripts and variants of the mouse genome. Probes were prepared and hybridization performed as described in the Two-Color Microarray Based Gene Expression Analysis Manual V. 6.5 (Agilent Technologies). Briefly, for each hybridization, 300 ng Cy3 probes and 300 ng Cy5 probes were mixed and added to 5 μl 10x Blocking Agent, 1 μl 25x Fragmentation Buffer and nuclease-free water in a 25 μl reaction, incubated (60ºC, 30 min) to fragment RNA, and the reaction terminated with 25 μl 2x Hybridization Buffer. Samples were placed on ice, quickly loaded onto arrays, hybridized in a hybridization oven rotator (65ºC, 17 h), then washed in GE Wash Buffer 1 (room temperature, 1 min) and in GE Wash Buffer 2 (37ºC, 1 min). Arrays were dried by centrifugation (2000 rpm, 2 min). Images were captured with an Agilent Microarray Scanner and spots quantified using Feature Extraction Software (Agilent Technologies). Microarray processing, hybridization and initial statistical analysis were performed by the Genomics Facility at the Centro Nacional de Biotecnología.

Sequences

For shRNA-*Dido1*, GIPZ lentiviral particles with the *Dido1*-specific target sequence CTCTCTGGGTGGTTCCTAA (Thermo Scientific).

For shRNA-*Wwp2*, retroviral vector pGFP-V-RS with four different 29mer shRNAs to murine *Wwp2* target sequences (Origene):
GTCAACCTCTCCAATGTCCTGAAGAACAA; GCACTTCAGCCAAAGATTCCTCTACCAGT; GTTCTGGCAGGTTGTCAAGGAGATGGACA; AAGGCTCACCTGGTGCCTATGACCGAAGT

For Q-PCR, *Dido* proximal promotor FW primer CGGAATCCGGTGCTGGTTTG; RV primer CATTTCCAGAGCTACCACGG; *Dido* intern side FW primer CTACACCTGGTTATCCACTGC; RV primer GCAGAGACCAACTCTTGCAAG

Peptide scan for epitope determination of MAB-1C6. Peptide scanning procedure to identify the epitope recognized by anti-DIDO MAB-1C6. A set of dodecapeptides consecutively shifted by two amino acids along the target sequence were synthesized automatically and linked directly to an activated membrane in a spot array. The target was the predicted amino acid sequence of mouse DIDO protein between positions 2-95. The membrane was blocked and analyzed by standard western blot, with digital imaging of chemiluminescent signal. MAB-1C6 specifically illuminated three spots that shared the HLSNEEAP sequence (residues 6-13 of murine DIDO protein).

Antibodies used in these experiments

Specificity	Antibody	Dilution	Source, reference	Technique
DIDO1	Rabbit polyclonal	1:400	Our laboratory, PAB-Dido1	IF
DIDO3	Rabbit polyclonal	1:400	Our laboratory, PAB-Dido3	IF
NT-DIDO	Mouse monoclonal	1:100	Our laboratory, Dido MAB-1C6	IF, WB
OCT4	Mouse monoclonal	1:100 1:1000	Santa Cruz, sc-5279	IF WB
GATA4	Goat polyclonal	1:200	R&D Systems	IF
HA-tag	Mouse monoclonal	1:500 1:1000	Covance, MMS-101P	IF WB
HA-tag	Rabbit polyclonal	1:1000 3-5 μg	Abcam; ChIP grade ab9110	IF, WB IP
FOCA2	Goat polyclonal	1:100	R&D Systems; af2400	IF
MEGALIN	Goat polyclonal	1:100	Santa Cruz; sc-16478	IF
aPKC	Rabbit polyclonal	1:200 1:2000	Santa Cruz; sc-216	IF WB
γ-TUBULIN	Mouse monoclonal	1:1000	Sigma-Aldrich; T6557	IF
γ-TUBULIN	Rabbit polyclonal	1:1000	Sigma-Aldrich; T3320	IF
acetylated-TUBULIN	Mouse monoclonal	1:400 1:2000	Sigma-Aldrich; T7451	IF WB
αβ-TUBULIN	Mouse monoclonal	1:500	Abcam; ab44928)	IF
WWP2	Rabbit polyclonal	1:200 5 μg	Bethyl; A302-936A	IF IP
WWP2	Goat polyclonal	1:200	Santa Cruz; sc-11896	WB
β-ACTIN	Mouse monoclonal	1:3000	Sigma-Aldrich; A3853	WB
EZRIN	Rabbit polyclonal	1:200	Cell Signalling; 3145	IF
RNAPOL II	Rabbit polyclonal	1:1000 1 μg	Santa Cruz; sc-899	WB IP
F-ACTIN	Phalloidin	1:500	Invitrogen; A 12381	IF
Nucleus	DAPI counterstain	1:300	Invitrogen; D 1306	

IF, immunofluorescence; WB, Western blot; IP, immunoprecipitation

Phosphopeptide analysis by LC-MS/MS ion trap

Phosphopeptide purification. The enrichment procedure concatenates two in-house-packed microcolumns, the immobilized metal affinity chromatography (IMAC) microcolumn and the Oligo R3 reverse-phase column, which provide selective purification and sample cleanup, respectively, prior to LC-MS/MS analysis. LC-MS/MS was performed as reported (Navajas et al., 2011).

Analysis by LC-MS/MS ion trap, alternating CID/ETD fragmentation techniques (collision-induced dissociation, CID;, electron transfer dissociation, ETD). Reverse-phase liquid chromatography was performed on an Ultimate 3000 nanoHPLC (Dionex, Amsterdam, The Netherlands). A 5 μl volume of reconstituted peptide sample was injected on a C18 PepMap trap column (5 μm, 100 Å, 300 μm ID x 5 mm) at a 30 μl/min flow rate, using H_2O:AcN:TFA (98:2:0.1) as loading mobile phase (5 min). The trap column was then switched on-line in back-flush mode to a C18 PepMap 100 analytical column (3 μm, 100 Å, 75 μm ID x 15 cm).

The micropump provided a 300 nl/min flow-rate and was operated in gradient elution conditions, using 0.1% formic acid in water as mobile phase A, and 0.1% formic acid in 80% acetonitrile/20% water as mobile phase B. Gradient elution conditions were as follows: isocratic conditions of 4% B (5 min), a linear increase to 50% B (in 60 min), a linear increase to 95% B (2 min), isocratic conditions of 95% B (4 min), and return to initial conditions in 2 min. The column was re-equilibrated for 15 min. Wavelengths were monitored at 214 and 280 nm with a UV detector.

NanoHPLC was coupled to a 3D ion trap mass spectrometer Amazon speed (Bruker Daltonics, Bremen, Germany) via CaptiveSpray ion source operating in positive ion mode, with capillary voltage set at 1.3 kV. The ion trap mass spectrometer was operated in a data-dependent mode, performing full scan (m/z 350-1500) MS spectra followed by tandem MS, alternating CID/ETD fragmentation of the eight most abundant ions. Dynamic exclusion was applied to prevent the same m/z from being isolated for 0.2 min after its fragmentation. For peptide identification, CID and ETD spectra were validated manually.

Chromatin-IP sequencing. DNA amount was determined by Picogreen and fragment size in a Bioanalyzer; fragments were within expected size distribution (125-325 bp). Libraries were generated from 5-10 ng DNA with Trueseq DNA Sample Preparation kit (Illumina) following the manufacturer's protocol, with modifications: no in-line control, Ampure purification step was replaced by purification with MinElute

(Qiagen); adaptor ligation with 1/100 adaptor dilution, PCR for enrichment of DNA fragments with 15 cycles. For high-throughput sequencing we used Illumina Sequencing Technology on an Illumina Genome Analyzer II (all steps performed by the Genomic Service Unit, Parque Científico de Madrid).

Bioinformatics analysis

Statistical analysis of Affymetrix microarray data

For analyses, we used the affylmGUI R package (Wettenhall *et al*., 2006). The robust multiarray analysis (RMA) algorithm was used for background correction, normalization and expression level summarization (Irizarry *et al*., 2003). This was followed by differential expression analysis with Bayes t-statistics from the linear models for microarray data (Limma) included in the affylmGUI package (Smyth, 2004; Smyth and Speed, 2003). P-values were corrected for multiple testing using the Benjamini-Hochberg method (Benjamini and Hochberg, 1995) and false discovery rate (Reiner *et al*., 2003). Genes were considered to be differentially expressed if the FDR was <0.2 (all selected probes with p-values <0.05). In addition, only probes with a fold-change variation >2 were considered for further analysis.

Statistical analysis of Agilent microarray data

Analysis was performed using the Limma and the non-parametric algorithm 'Rank Products' packages available at Bioconductor (Huber *et al*., 2015). P-values were corrected for multiple testing using the Benjamini-Hochberg method and FDR. Genes were considered differentially expressed and selected for further study when the Limma FDR was <0.2 (all selected probes with adjusted p-values <0.05) and a 2-fold change difference was found in expression values.

Statistical analysis of ChIP-seq

DNA from immunoprecipitated chromatin was sequenced in a GAII Illumina sequencer. Sequences in FASTQ format were mapped to the mouse genome (NCBI Build 37/UCSC mm9) using BOWTIE aligner (bowtie2 v2.0.6; (Langmead and Salzberg, 2012). Resulting BAM files were transformed into SAM format with Samtools (v1.3.1. view, sort, index; (Li et al., 2009) and resulting SAM files were used to define binding regions. Peak calling software MACS (v1.4; (Zhang et al., 2008) was used to identify significant peaks by comparing experimental IP and input control data with default parameters (band width = 300, model fold = 10,30, p-value cutoff = 1.00e-05). A total of 2888 significant peaks were finally called.

Other ChIP-seq data

From (Brookes et al., 2012):
GEO accession data - GSE34520

-RNApolIInoP-GSM850469_RNAPII_8WG16.bw
-RNApolIIS5P-GSM850467_RNAPII_S5P.bw
-RNApolIIS2P-GSM850470_RNAPII_S2P.bw
-RNApolIIS7P-GSM850468_RNAPII_S7P.bw

Bing Ren, Ph.D. http://bioinformatics-renlab.ucsd.edu/rentrac/
and
An integrated encyclopedia of DNA elements in the human genome.
ENCODE Project Consortium. Nature. 2012 Sep 6;489(7414):57-74. doi: 10.1038/nature11247.

H3K4me3	https://www.encodeproject.org/files/ENCFF001KEH
H3K9ac	https://www.encodeproject.org/files/ENCFF001KDA
H3K27ac	https://www.encodeproject.org/files/ENCFF001KDN
H3K4me1	https://www.encodeproject.org/files/ENCFF001KEH
H3K36me3	https://www.encodeproject.org/files/ENCFF001KDY
H3K27me3	https://www.encodeproject.org/files/ENCFF001KDS
H3K9me3	https://www.encodeproject.org/files/ENCFF001KDG

Further post-processing analysis

FIESTA viewer (http://bioinfogp.cnb.csic.es/tools/FIESTA/index_server.php) was used for data visualization of microarray data (Oliveros, 2007). The Integrative Genomics Viewer (IGV, http://www.broadinstitute.org/igv) (Robinson et al., 2011) (Thorvaldsdottir et al., 2013) was used for visualization and exploration of genomic datasets. MeV (MultiExperiment Viewer (http://www.tm4.org/mev.html) (Saeed *et al*., 2003) was used for gene clustering of Agilent microarray data. For clustering, first a list of significant probes was obtained for any of the three conditions tested (2403 probes). Probes with no change (<1.5-fold change) in control vs Dido3ΔCT condition were removed. The resulting probe list (1531 probes) was passed to the MeV application and HCL clustering was performed (Eisen *et al*., 1998). Probes were then manually assigned to six distinct gene expression profile groups and individual probe lists for each group were analyzed for Gene Ontology biological process enrichments online in the DAVID website, using mouse annotations as background for comparison (DAVID Bioinformatics Resources 6.7, https://david.ncifcrf.gov/home.jsp; (Huang da et al., 2009a, b).

Supplemental References

Benjamini, Y., and Hochberg, Y. (1995). Controling the false discovery rate: a practical and powerful approach to multiple testing. J Roy Stat Soc B 57, 289-300.

Brookes, E., de Santiago, I., Hebenstreit, D., Morris, K.J., Carroll, T., Xie, S.Q., Stock, J.K., Heidemann, M., Eick, D., Nozaki, N., et al. (2012). Polycomb associates genome-wide with a specific RNA polymerase II variant, and regulates metabolic genes in ESCs. Cell Stem Cell 10, 157-170.

Eisen, M.B., Spellman, P.T., Brown, P.O., and Botstein, D. (1998). Cluster analysis and display of genome-wide expression patterns. Proc Natl Acad Sci USA 95, 14863-14868.

ENCODE Project Consortium. An integrated encyclopedia of DNA elements in the human genome. Nature. 2012 Sep 6;489(7414):57-74.

Huang da, W., Sherman, B.T., and Lempicki, R.A. (2009a). Bioinformatics enrichment tools: paths toward the comprehensive functional analysis of large gene lists. Nucleic Acids Res 37, 1-13.

Huang da, W., Sherman, B.T., and Lempicki, R.A. (2009b). Systematic and integrative analysis of large gene lists using DAVID bioinformatics resources. Nat Protoc 4, 44-57.

Huber, W., Carey, V.J., Gentleman, R., Anders, S., Carlson, M., Carvalho, B.S., Bravo, H.C., Davis, S., Gatto, L., Girke, T., et al. (2015). Orchestrating high-throughput genomic analysis with Bioconductor. Nat Methods 12, 115-121.

Irizarry, R.A., Hobbs, B., Collin, F., Beazer-Barclay, Y.D., Antonellis, K.J., Scherf, U., and Speed, T.P. (2003). Exploration, normalization, and summaries of high density oligonucleotide array probe level data. Biostatistics 4, 249-264.

Langmead, B., and Salzberg, S.L. (2012). Fast gapped-read alignment with Bowtie 2. Nat Methods 9, 357-359.

Li, H., Handsaker, B., Wysoker, A., Fennell, T., Ruan, J., Homer, N., Marth, G., Abecasis, G., Durbin, R., and Genome Project Data Processing, S. (2009). The Sequence Alignment/Map format and SAMtools. Bioinformatics 25, 2078-2079.

Navajas, R., Paradela, A., and Albar, J.P. (2011). Immobilized metal affinity chromatography/reversed-phase enrichment of phosphopeptides and analysis by CID/ETD tandem mass spectrometry. Methods Mol Biol 681, 337-348.

Oliveros, J.C. (2007). FIESTA@BioinfoGP. An interactive server for analyzing DNA microarray experiments with replicates (http://bioinfogp.cnb.csic.es/tools/FIESTA).

Reiner, A., Yekutieli, D., and Benjamini, Y. (2003). Identifying differentially expressed genes using false discovery rate controlling procedures. Bioinformatics 19, 368-375.

Robinson, J.T., Thorvaldsdottir, H., Winckler, W., Guttman, M., Lander, E.S., Getz, G., and Mesirov, J.P. (2011). Integrative genomics viewer. Nat Biotechnol 29, 24-26.

Saeed, A.I., Sharov, V., White, J., Li, J., Liang, W., Bhagabati, N., Braisted, J., Klapa, M., Currier, T., Thiagarajan, M., et al. (2003). TM4: a free, open-source system for microarray data management and analysis. Biotechniques 34, 374-378.

Smyth, G.K. (2004). Linear models and empirical bayes methods for assessing differential expression in microarray experiments. Stat Appl Genet Mol Biol 3, Article3.

Smyth, G.K., and Speed, T. (2003). Normalization of cDNA microarray data. Methods 31, 265-273.

Thorvaldsdottir, H., Robinson, J.T., and Mesirov, J.P. (2013). Integrative Genomics Viewer (IGV): high-performance genomics data visualization and exploration. Brief Bioinform 14, 178-192.

Trachana, V., van Wely, K.H., Guerrero, A.A., Futterer, A., and Martinez, A.C. (2007). Dido disruption leads to centrosome amplification and mitotic checkpoint defects compromising chromosome stability. Proc Natl Acad Sci USA 104, 2691-2696.

Wettenhall, J.M., Simpson, K.M., Satterley, K., and Smyth, G.K. (2006). affylmGUI: a graphical user interface for linear modeling of single channel microarray data. Bioinformatics 22, 897-899.

Zhang, Y., Liu, T., Meyer, C.A., Eeckhoute, J., Johnson, D.S., Bernstein, B.E., Nusbaum, C., Myers, R.M., Brown, M., Li, W., et al. (2008). Model-based analysis of ChIP-Seq (MACS). Genome Biol 9, R137.